

**AFRL-VA-WP-TP-2003-301**

**COMPARISON OF PREDICTED AND  
MEASURED FORMATION FLIGHT  
INTERFERENCE EFFECTS**



**William B. Blake  
David R. Gingras**

**AUGUST 2001**

**Approved for public release; distribution is unlimited.**

**This material is declared a work of the U.S. Government and is not subject to copyright protection in the United States.**

**AIR VEHICLES DIRECTORATE  
AIR FORCE RESEARCH LABORATORY  
AIR FORCE MATERIEL COMMAND  
WRIGHT-PATTERSON AIR FORCE BASE, OH 45433-7542**

<b>REPORT DOCUMENTATION PAGE</b>				<i>Form Approved</i> <i>OMB No. 0704-0188</i>	
<p>The public reporting burden for this collection of information is estimated to average 1 hour per response, including the time for reviewing instructions, searching existing data sources, gathering and maintaining the data needed, and completing and reviewing the collection of information. Send comments regarding this burden estimate or any other aspect of this collection of information, including suggestions for reducing this burden, to Department of Defense, Washington Headquarters Services, Directorate for Information Operations and Reports (0704-0188), 1215 Jefferson Davis Highway, Suite 1204, Arlington, VA 22202-4302. Respondents should be aware that notwithstanding any other provision of law, no person shall be subject to any penalty for failing to comply with a collection of information if it does not display a currently valid OMB control number. <b>PLEASE DO NOT RETURN YOUR FORM TO THE ABOVE ADDRESS.</b></p>					
<b>1. REPORT DATE (DD-MM-YY)</b> August 2001		<b>2. REPORT TYPE</b> Conference Paper		<b>3. DATES COVERED (From - To)</b>	
<b>4. TITLE AND SUBTITLE</b> COMPARISON OF PREDICTED AND MEASURED FORMATION FLIGHT INTERFERENCE EFFECTS				<b>5a. CONTRACT NUMBER</b> F33615-99-C-3002	
				<b>5b. GRANT NUMBER</b>	
				<b>5c. PROGRAM ELEMENT NUMBER</b> 65502F	
<b>6. AUTHOR(S)</b> William B. Blake (AFRL/VACA) David R. Gingras (Bihrl Applied Research)				<b>5d. PROJECT NUMBER</b> 3005	
				<b>5e. TASK NUMBER</b> 40	
				<b>5f. WORK UNIT NUMBER</b> L2	
<b>7. PERFORMING ORGANIZATION NAME(S) AND ADDRESS(ES)</b> Control Theory Optimization Branch (AFRL/VACA) Control Sciences Division Air Vehicles Directorate Air Force Research Laboratory, Air Force Materiel Command Wright-Patterson Air Force Base, OH 45433-7542				<b>8. PERFORMING ORGANIZATION REPORT NUMBER</b> AIAA 2001-4136	
<b>9. SPONSORING/MONITORING AGENCY NAME(S) AND ADDRESS(ES)</b> Air Vehicles Directorate Air Force Research Laboratory Air Force Materiel Command Wright-Patterson Air Force Base, OH 45433-7542				<b>10. SPONSORING/MONITORING AGENCY ACRONYM(S)</b> AFRL/VACA	
				<b>11. SPONSORING/MONITORING AGENCY REPORT NUMBER(S)</b> AFRL-VA-WP-TP-2003-301	
<b>12. DISTRIBUTION/AVAILABILITY STATEMENT</b> Approved for public release; distribution is unlimited.					
<b>13. SUPPLEMENTARY NOTES</b> AIAA Atmospheric Flight Mechanics Conference Paper, AIAA-2001-4136, August 2001. This material is declared a work of the U.S. Government and is not subject to copyright protection in the United States. Report contains color.					
<b>14. ABSTRACT (Maximum 200 Words)</b> Results from a wind tunnel test of two delta wings in close proximity are presented and compared with predictions from a vortex lattice method. The wake effects on lift are slightly overpredicted when the aircraft overlap in the spanwise direction. The wake induced effects on pitching and rolling moment are well predicted. A maximum induced drag reduction of 25% is measured on the trail aircraft, compared with a 40% predicted reduction.					
<b>15. SUBJECT TERMS</b>					
<b>16. SECURITY CLASSIFICATION OF:</b>			<b>17. LIMITATION OF ABSTRACT:</b> SAR	<b>18. NUMBER OF PAGES</b> 18	<b>19a. NAME OF RESPONSIBLE PERSON (Monitor)</b> William B. Blake <b>19b. TELEPHONE NUMBER (Include Area Code)</b> (937) 255-6764
<b>a. REPORT</b> Unclassified	<b>b. ABSTRACT</b> Unclassified	<b>c. THIS PAGE</b> Unclassified			

COMPARISON OF PREDICTED AND MEASURED FORMATION FLIGHT INTERFERENCE EFFECTS

William B. Blake \*  
 Air Force Research Laboratory  
 Wright Patterson AFB OH 45433-7531

David R. Gingras \*\*  
 Bihrl Applied Research  
 Hampton VA 23666

ABSTRACT

Results from a wind tunnel test of two delta wings in close proximity are presented and compared with predictions from a vortex lattice method. The wake effects on lift are slightly overpredicted when the aircraft overlap in the spanwise direction. The wake induced effects on pitching and rolling moment are well predicted. A maximum induced drag reduction of 25% is measured on the trail aircraft, compared with a 40% predicted reduction.

NOMENCLATURE

A	Aspect ratio
b	Wing span
$C_A$	Axial force coefficient
$C_L$	Lift coefficient
$C_D$	Drag coefficient
$C_{D_0}$	Zero lift drag coefficient
$C_{D_i}$	Induced drag coefficient
$C_l$	Rolling moment coefficient
$C_m$	Pitching moment coefficient
$C_N$	Normal force coefficient
$K_{ij}$	Induced drag factor
x	Longitudinal distance, Fig 2
y	Lateral distance, Fig 2
z	Vertical distance, Fig 2
$\alpha$	Angle of attack

\* Aerospace Engineer, Associate Fellow AIAA  
 \*\* Aerospace Engineer, Senior Member AIAA

This paper is declared a work of the U.S. government and is not subject to copyright protection in the United States.

INTRODUCTION

Many military missions involve formation flight. In some instances, there is significant aerodynamic coupling between aircraft arising from the proximity of one aircraft to wakes generated by others in the formation. While aerial refueling is the most common example, a new one is currently under study, formation flight for drag reduction. This is now considered practical due to the ability to determine aircraft location with high precision and advances in automatic control theory. If the aircraft are appropriately positioned, upwash from wing tip vortices can reduce the drag of neighboring aircraft, increasing range or endurance<sup>1</sup>. It is generally accepted that this drag reduction is one of the reasons that many migratory bird species fly in closely spaced flocks<sup>2</sup>. Photographic studies of Canadian Geese have found that the average lateral spacing between adjacent birds is very close to the optimum predicted by simple aerodynamic theory<sup>3</sup>.

Most of the research in this area has concentrated on analytical modeling using potential flow techniques<sup>4,5</sup>. Very few experimental results are reported in the open literature. Brown et al<sup>6</sup> conducted tow tank tests using a 3% scale Boeing 747 model as the wake generator and a generic fighter as the trail aircraft. The trail to lead aircraft wing span ratio was 0.20. Forces were measured on the trail aircraft only, with lift-to-drag ratio increases of up to 50% measured at some conditions. Beukenberg and Hummel<sup>7</sup> conducted two flight tests in an attempt to demonstrate a power saving under realistic conditions. In their

second test, a Dornier-228 acted as a vortex generator for a following Dornier-28. Using an automatic control system to maintain proper position, an average power reduction of 10% was measured on the trail aircraft over a 150 sec. interval.

There have been many wind tunnel tests studying the impact of wake vortices on aircraft far downstream. Most of these center on the study of wake vortex hazards for commercial aircraft and are conducted in large facilities such as the 80x120 tunnel at the NASA Ames Research Center<sup>8</sup> or the 30x60 facility at the Langley Research Center<sup>9</sup>. Bloy et al<sup>10</sup> investigated formations typical of aerial refueling with the receiver less than one wing span downstream of the tanker. Their tests were conducted in a small wind tunnel with a relatively large wing span to tunnel width ratio of 0.7. Significant wall interference effects were uncovered by taking measurements in both open and closed test sections.

The flow survey rig within the Langley 30x60 Full Scale Wind Tunnel has recently been modified to accommodate an aircraft model with an internal force balance al<sup>11</sup>. The present work discusses test results from a formation of two closely spaced tailless aircraft using this rig and compares these with predictions from a vortex lattice method.

## DISCUSSION

### WIND TUNNEL SET-UP

The wind tunnel tests were conducted in the Langley Full Scale Wind Tunnel, currently operated by Old Dominion University. The test configuration was a Lockheed tailless aircraft consisting of a 65 degree delta wing with a sawtooth trailing edge with sweep angles of  $\gamma$  25 degrees. It is a single engine design with a two narrow inlets on the lower surface. The inlets were blocked for the present test.

Two 1/13 scale models were tested. These were manufactured several years apart by different firms, so slight differences are present. They will be referred to as models “A” and “B”. Model B was manufactured later and has several bumps and exposed rods to accommodate internally actuated

control surfaces. Model B was used as the trail model during all of the formation tests, and was mounted using an aft sting which was connected to a vertical rod. This rod was connected to the wind tunnel’s primary model support system. Model A was mounted from the top on a newly built apparatus which was attached to the existing flow survey carriage. The apparatus consists of an arm which projects forward of the survey carriage, under which a vertical sting and angle of attack control rod are attached. This arrangement was selected in an attempt to minimize rig interference effects on model B. A photograph of the experimental apparatus is shown in Figure 1.



FIGURE 1. Wind Tunnel Models on Apparatus

The relative height of the two models was achieved by varying the position of Model B. This was accomplished by moving the sting along the vertical rod which was attached to the primary support system. Relative lateral and longitudinal position were achieved by moving the flow survey rig to which Model A was attached. All runs were conducted at a tunnel dynamic pressure of 5 psf, which corresponds to a speed of approximately 65 ft/sec.

Both models were equipped with internal six component strain gauge balances. The estimated accuracy of the balance measurements, based on pretest balance calibrations expressed in non-dimensional form using the reference area and length of the study vehicle is presented in Table 1.

$\Delta C_N$	$\Delta C_A$	$\Delta C_m$	$\Delta C_l$
$\gamma 0.004$	$\gamma 0.004$	$\gamma 0.008$	$\gamma 0.0006$

Additional details on the experimental set-up and data reduction are given by Gingras<sup>11</sup>.

## PREDICTION METHOD

The planar vortex lattice code HASC95<sup>12</sup> was used to predict the wake induced effects on the trail aircraft. Each aircraft was modeled with 540 panels, using 36 in the spanwise direction and 15 in the chordwise direction. The spanwise panels were evenly spaced, cosine spacing was used for the chordwise elements. Care was taken to ensure correct alignment of vortex filaments and control points when the aircraft overlapped in the lateral direction. HASC95 uses the flat wake approximation, i.e., the trailing vortex legs extend to infinity parallel to the x-y plane, and do not vary with angle of attack. One result of this is that in the linear lift region, the wake induced lift, rolling moment and pitching moment increments are invariant with the angle of attack of the trail aircraft. The HASC95 representation of the vehicles is shown in Figure 2.

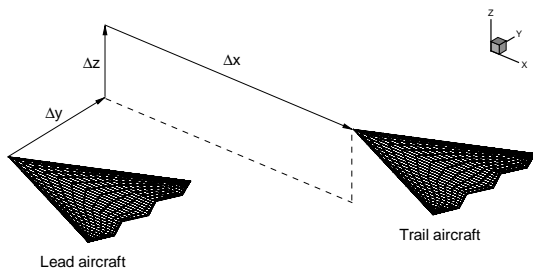


FIGURE 2. Vortex Lattice Representation of Vehicles

Rosow<sup>13</sup> has shown that the vortex lattice method is extremely accurate for predicting wake induced effects when the span of the downstream wing is substantially less than that of the wake generating wing. When the spans of the two wings are comparable, as in the present tests, accuracy was degraded somewhat but trends were still very well predicted. The reduction in accuracy was attributed to distortions of the wake cause by the presence of the downstream wing. Bloy et al<sup>13</sup> also found good agreement with vortex lattice predictions when compared to their open test section results.

## ISOLATED MODEL RESULTS

The lift coefficient of models A and B in isolation is shown in Figure 3, along with the HASC95 prediction. For the formation flight tests, model A used a top mounted sting and model B used an aft mount. Model A was tested in isolation using both aft and top mounts to assess sting effects and allow comparison with prior tests which used an aft mounted sting. Also shown are data from two prior tests<sup>14,15</sup> of model A using an aft mounted sting. This was the first test with model B. The differences between the models are at least as large as any facility or mounting effects. Model B on the aft mount has slightly higher lift than any of the model A results. The HASC95 prediction is very good below 10 degrees angle of attack and is slightly low at higher angles of attack.

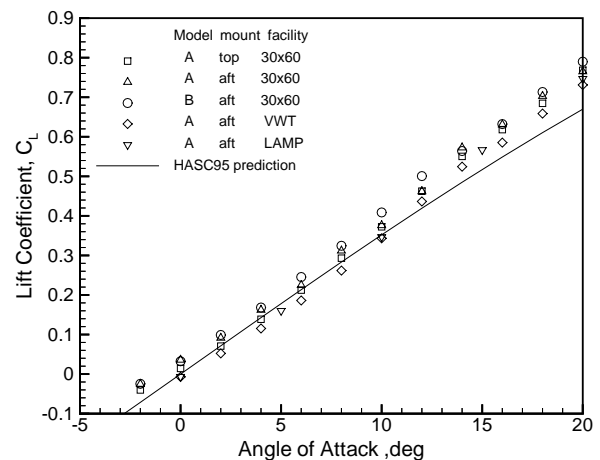


FIGURE 3. Lift of Models in Isolation

Drag characteristics of the models in isolation, along with HASC95 predictions, are shown in Figure 4. The two models show very similar results, with Model A having a slightly larger zero lift drag than model B. The experimentally measured zero lift drag of model B was added to the HASC95 prediction. Three predictions are shown, corresponding to three levels of assumed leading edge suction, or flow attachment. Full leading edge suction corresponds to a fully attached flow condition, with:

$$C_{Di} = C_L^2 / \pi A$$

Zero leading edge suction corresponds to a fully separated flow condition, with:

$$C_{Di} = C_L \tan \alpha$$

At low lift coefficients, the drag compares well with the full suction prediction. As lift increases, some

flow separation is evident due to the rise in drag above the full suction prediction. The drag never reaches the value corresponding to fully separated flow case. Several values of suction were run in an attempt to match the value measured at 8 degrees angle of attack, which is the reference case for most of the formation flight effects. A value of 60% attained suction gives a very good match, as shown.

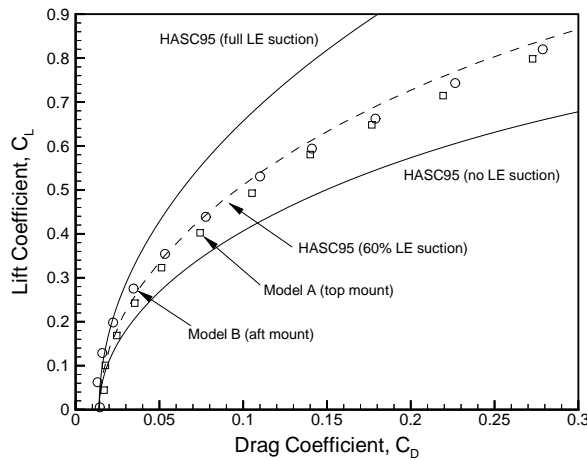


FIGURE 4. Drag Polars of Models in Isolation

## FORMATION FLIGHT RESULTS

### LATERAL SPACING – LIFT AND DRAG

The effect of lateral spacing on the wake induced lift is shown in Figure 5. These results are for a longitudinal spacing of two spans and zero vertical spacing (aircraft in the same plane relative to the oncoming wind). The lead aircraft is at eight degrees angle of attack in all cases. Results are shown for the trail aircraft at zero and eight degrees angle of attack. Maximum lift loss occurs with the aircraft directly in trail when it is completely enveloped by the downwash from the lead. As the trail aircraft moves outboard, the lift loss reduces and upwash is encountered which reduces once the trail aircraft has passed the lead’s wing tip ( $y/b > 1$ ).

The HASC95 prediction shows the correct trend, and the magnitude of the lift is well predicted for lateral spacings greater than 2/3 span. The lift loss is underpredicted for smaller spacings. This may be due to a reduction in local dynamic pressure immediately behind the lead aircraft, which HASC95 ignores. The wake induced lift is not

affected by the angle of attack of the trail vehicle. This is consistent with the HASC95 results.

Lift-to-drag ratio as a function of lift for several lateral spacings is shown in Figure 6. The aircraft in isolation is shown as the solid line, with formation flight results shown as dashed lines. These data were taken from angle of attack sweeps of the trail aircraft with the lead at a fixed angle of attack. Drag reduction comparisons are most meaningful for the case where both aircraft are at the same lift coefficient. Here, a drag reduction of almost 15% is attained for the trail aircraft.

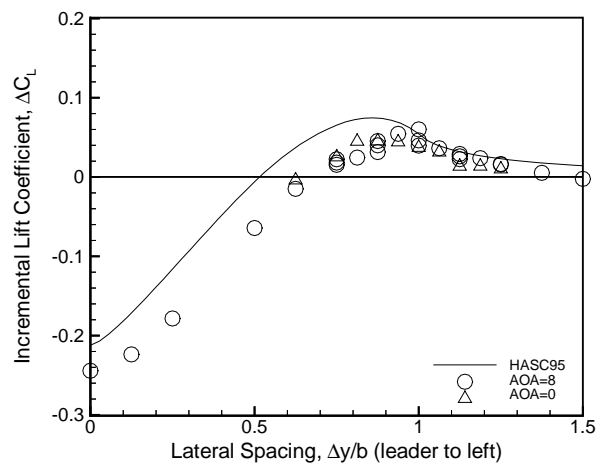


FIGURE 5. Effect of lateral spacing on wake induced lift,  $x/b=2$ ,  $z/b=0$ .

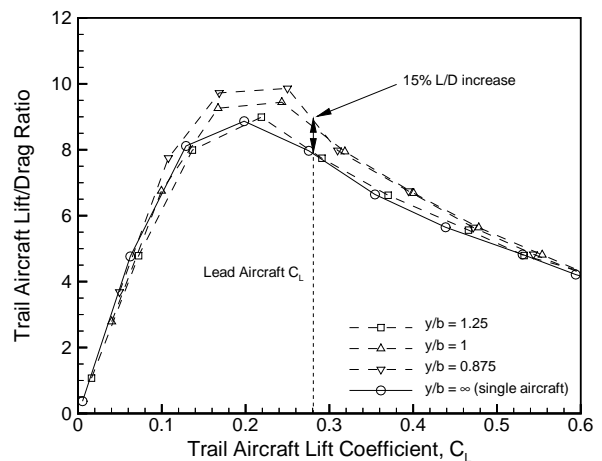


FIGURE 6. Formation flight lift-to-drag characteristics,  $x/b=2$ ,  $z/b=0$ .

In the HASC95 runs, both aircraft are at the same angle of attack, so the lift of the two vehicles is almost always different. Prandtl’s method<sup>16</sup> was

used to extract the induced drag effect for cases of differing lift on the lead and trail wings:

$$C_{D,2} = C_{D,o} + K_o C_{L,2}^2 + K_{12} C_{L,1} C_{L,2}$$

Here,  $K_o$  represents the self induced drag and  $K_{12}$  represent the effect of wing 1 on wing 2. The induced drag change due to formation effects can be easily calculated:

$$\frac{K_{12}}{K_o} = \frac{C_{L,2}}{C_{L,1}} \left[ \frac{C_{D,2} - C_{D,o}}{K_o C_{L,2}^2} - 1 \right]$$

The same procedure was used to extract the induced drag reduction from the experimental data.  $K_o$  was determined from a curve fit of the isolated aircraft lift and drag results. If two untapered wings are physically joined, the induced drag change of the added wing ( $K_{12}/K_o$ ) is  $-1$  or 100% reduction. The HASC95 results for the fully attached flow case (dashed curve) indicate a maximum reduction of about 70% at a spacing of 90% span, indicating a slight overlap of the wings. Simple horseshoe vortex theory predicts a maximum reduction of 100% at  $\pi/4$  (78%) span. The reduction is smaller for the present case due to the high degree of wing taper. The HASC95 results for 60% attained suction show a predicted drag reduction of 40%, also occurring at 90% span spacing. The test data show a maximum reduction of about 25%, occurring between 80 and 90 % span spacing. Although the overall trend of the data matches the prediction, the reduction is about 15% less than predicted across the board. One possible explanation for this discrepancy is that the induced velocities at the trail aircraft wing tip are high enough to significantly increase flow separation. Using a pair of fully rolled up vortices to represent the wake, the estimated induced upwash angle at the tip of the trail aircraft is 8 degrees for the present test conditions. Added to the geometric angle of attack of 4-10 degrees, this almost certainly increases separation.

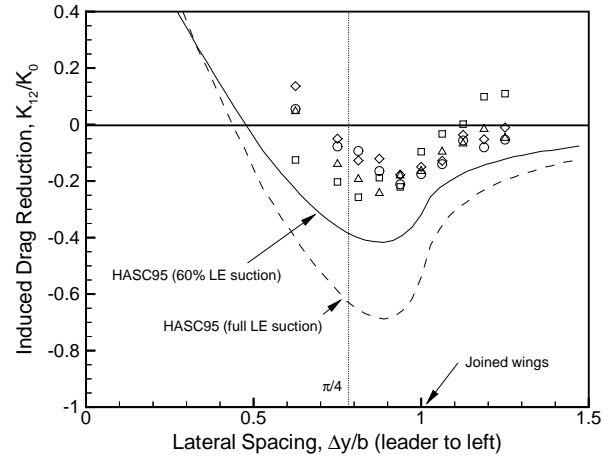


FIGURE 7. Effect of lateral spacing on induced drag reduction,  $x/b=2$ ,  $z/b=0$ .

### LATERAL SPACING – PITCH AND ROLL

The effect of lateral spacing on the wake induced pitching moment is shown in Figure 8. For reference, a maximum (30 degree) elevon deflection gives a pitching moment increment of  $-0.040$ , so the maximum induced moment corresponds to about a 50% control deflection. There are three distinct peaks in the incremental moment, occurring at approximately one-quarter span, two-thirds span, and wingtip spacing. HASC95 does an excellent job of predicting the size and location of these peaks.

The pitching moment data in figure 8 show a small effect of angle of attack when the wings overlap ( $y/b < 1$ ), with an increased nose up moment with angle of attack. The zero angle of attack data is more accurately predicted by HASC95. If it is assumed that the wake from the lead is parallel to the velocity vector, then at zero angle of attack the trail aircraft is perfectly aligned with the lead's wake, which is the HASC95 representation.

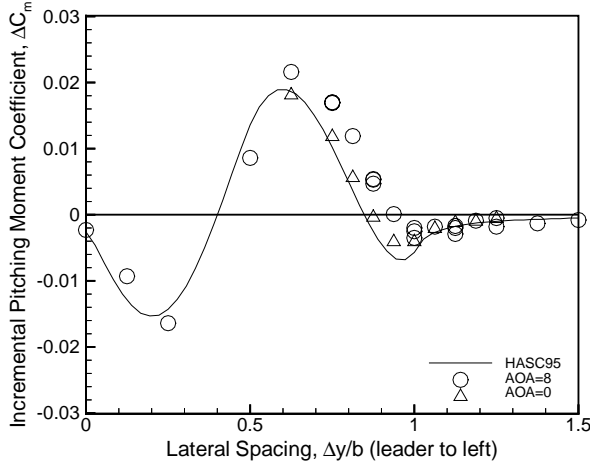


FIGURE 8. Effect of lateral spacing on wake induced pitching moment,  $x/b=2$ ,  $z/b=0$ .

To examine the changes in sign of the pitching moment result, pressure distributions were obtained from HASC95. These are shown for lateral spacings of 1/3 and 2/3 span in Figure 9 and 10. They were obtained by subtracting the pressures of an isolated vehicle at eight degrees angle of attack from the pressures of both vehicles while in formation. Dashed curves indicate regions of downwash while solid lines represent upwash. The contours are shown at increments of 0.02 in terms of  $C_p$ . Although there is a small effect of the trail aircraft on the lead, it cannot be seen at this resolution in  $C_p$ . The black dots indicate the moment reference center.

Figure 9 shows a downwash region that is nearly aligned with the lead's right wing tip. The upwash is mostly aft of the moment center, with a large downwash at the nose. This results in the nose down moment shown in Figure 8. Figure 10 shows a small downwash region at the left wing tip of the trail, with only upwash forward of the moment reference center. This results in the maximum nose up moment peak shown in Figure 8. It is interesting to note that the approximate dividing line between downwash and upwash for the 2/3 span case is not aligned with the lead's wingtip, but with a point further inboard.

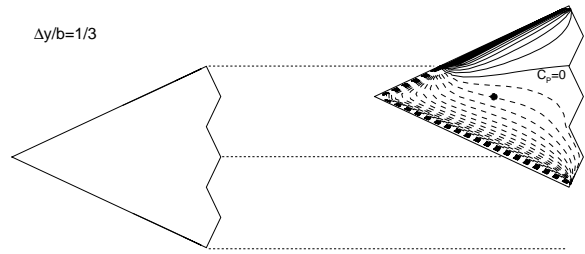


FIGURE 9. Wake induced pressure contours at  $y/b=1/3$ ,  $x/b=2$ ,  $z/b=0$ .

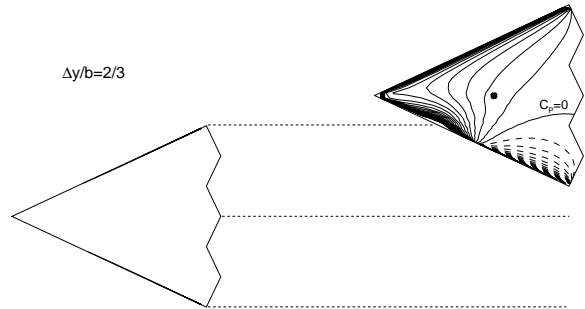


FIGURE 10. Wake induced pressure contours at  $y/b=2/3$ ,  $x/b=2$ ,  $z/b=0$ .

The effect of lateral spacing on the wake induced rolling moment lift is shown in Figure 11. For reference, a maximum (30 degree) elevon deflection gives a pitching moment increment of  $-0.022$ , so the maximum induced moment corresponds to about a 100% control deflection.

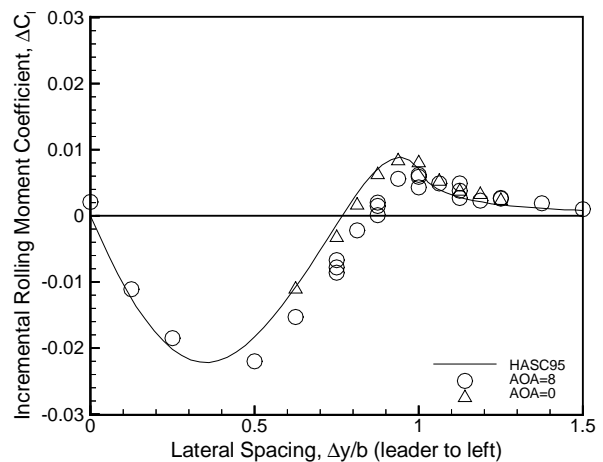


FIGURE 11. Effect of lateral spacing on wake induced rolling moment,  $x/b=2$ ,  $z/b=0$ .

## VERTICAL SPACING

The effect of vertical spacing on the wake induced lift is shown in Figure 12. Results are shown for a

longitudinal spacing of two spans and three lateral spacings, 0.25, 0.75 and 1.25 spans. Both the lead and trail aircraft are at eight degrees angle of attack. The scale of the vertical axis matches that shown for the lateral spacing comparisons. The trends are very well predicted, while the magnitudes are not. In all cases, the maximum lift changes correspond to the in-plane ( $\Delta z/b=0$ ). For some of the 0.75 span results, the same position was tested during multiple runs. These additional points are very close to one another, indicating good repeatability of the induced effects.

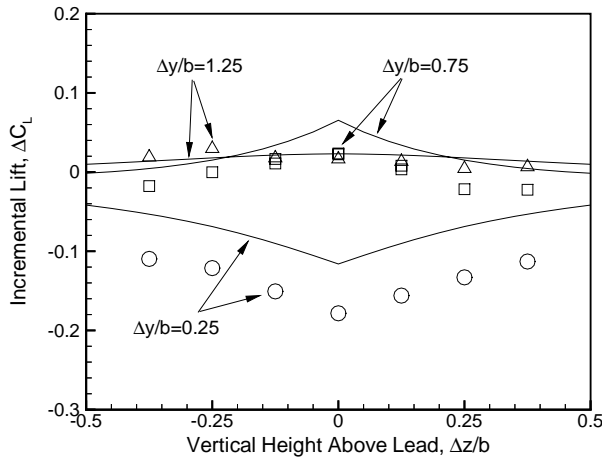


FIGURE 12. Effect of vertical spacing on wake induced lift,  $x/b=2$ .

The effect of vertical spacing on the wake induced pitching and rolling moments are shown in Figure 13-14. For the most part, as with the lift, the maximum changes occur for the in-plane case. The pitching moment results are very well predicted in all cases. The rolling moment results are well predicted for the 0.25 and 1.25 span spacing cases. For the 0.75 span case, the results are mixed. The data show a continually increasing moment with height, while the prediction shows virtually no effect of height.

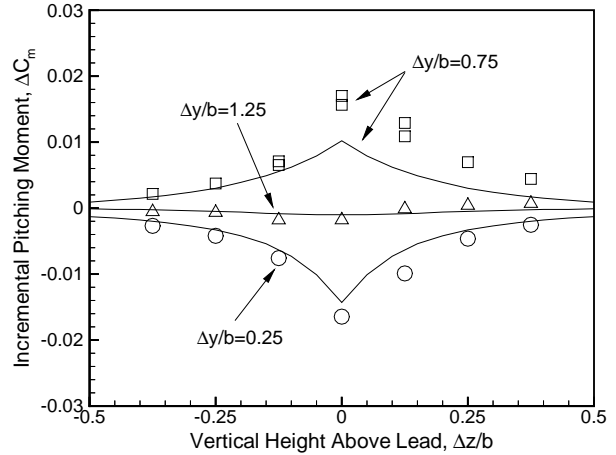


FIGURE 13. Effect of vertical spacing on wake induced pitching moment,  $x/b=2$ .

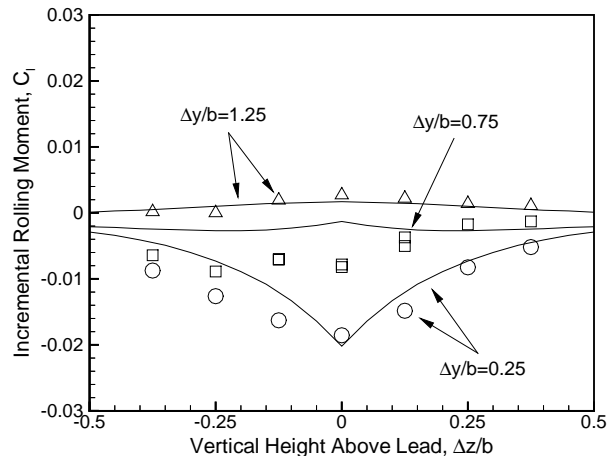


FIGURE 14. Effect of vertical spacing on wake induced pitching moment,  $x/b=2$ .

### POSITIONAL STABILITY

One important aspect of formation flight is positional stability. Positive stability results if the wake induced forces tend to return the trail aircraft to its original position when disturbed. About a dozen positional stability derivatives exist, many have been studied by Bloy et al<sup>10</sup>. For the current tests, three will be examined, change in lift and pitching moment with height, and change in roll with lateral separation. For the sign convention selected, these are stable for:

$$\frac{\partial C_L}{\partial z} < 0$$

$$\frac{\partial C_m}{\partial z} < 0$$

$$\frac{\partial C_l}{\partial y} < 0$$

Derivatives involving yawing moment and side force were effectively zero due to the tailless

configuration. Apparatus limitations prevented study of other derivatives such as change in roll with bank angle.

Stability boundaries for the change in lift with height derived from HASC95 results are shown in Figure 15. Boundaries extracted from the experimental data are shown in Figure 16. The HASC95 results are symmetric with respect to both the horizontal and vertical planes of symmetry of the lead aircraft. Sufficient data were only taken on one side of the aircraft to generate boundaries. As a result, results are only shown for the trail aircraft to the right of the lead. The experimentally measured boundaries should be symmetric with respect to the vertical plane of symmetry.

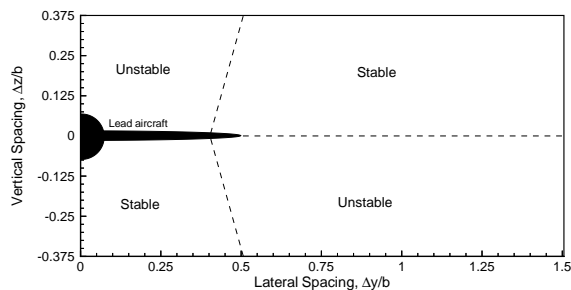


FIGURE 15. Predicted regions of positional stability in lift,  $x/b=2$ .

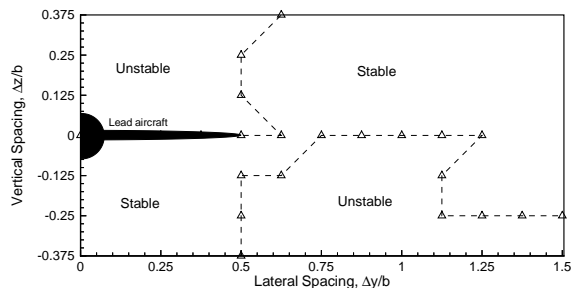


FIGURE 16. Measured regions of positional stability in lift,  $x/b=2$ .

HASC95 predicts four distinct regions of lift stability, stable in lift when behind and below the lead aircraft or to the side and above. These regions are divided by a 4-corner boundary, located at 0.40 span spacing. The data agree well with the predicted boundaries with two small exceptions. Instead of a 4-corner boundary between regions, the data show the region of positive stability to be continuous with a small channel present just outside the wing tip (0.6 span spacing). The data also show

a small stable region beneath the vertical plane of symmetry outboard of wingtip (1.0) spacing.

Stability boundaries for the change in pitching moment with height are shown in Figures 17 and 18. HASC95 predicts six distinct stability regions, which are separated by two 4-corner boundaries, located at 0.40 and 0.80 span spacing. The data show the same general trends as the prediction. As with the lift prediction, the data do not show 4-corner boundaries. Instead, the region of instability is continuous with channels separating the stable regions. In addition, the data show a small region of instability directly behind and below the aircraft that was not predicted. The Appendix gives a summary of the longitudinal dynamic modes of the aircraft in formation flight.

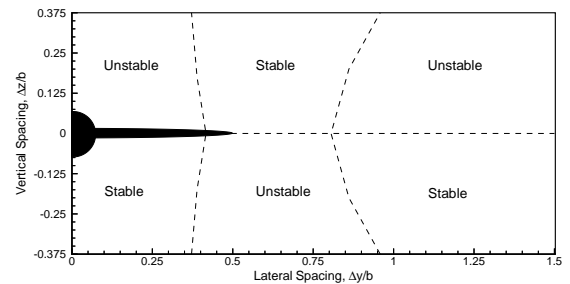


FIGURE 17. Predicted regions of positional stability in pitch,  $x/b=2$ .

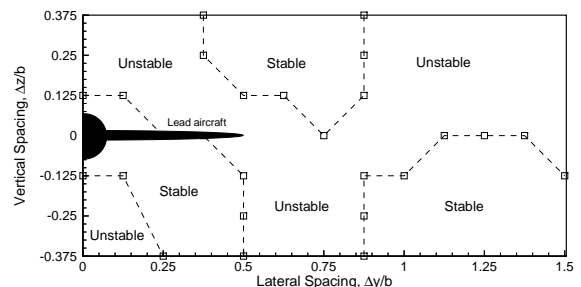


FIGURE 18. Measured regions of positional stability in pitch,  $x/b=2$ .

Stability boundaries for the change in rolling moment with lateral position are shown in Figures 19 and 20. HASC95 predicts three distinct stability regions. The boundaries of these regions in the horizontal plane of symmetry are located at 0.36 and 0.94 span spacing. The data agree very well with the prediction.

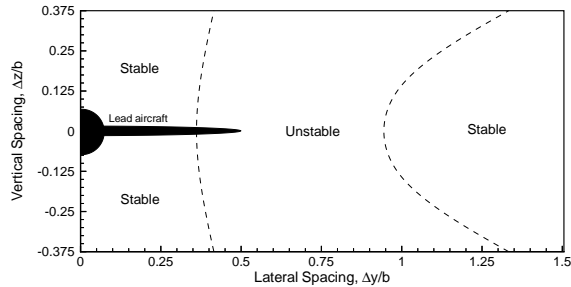


FIGURE 19. Predicted regions of positional stability in roll,  $x/b=2$ .

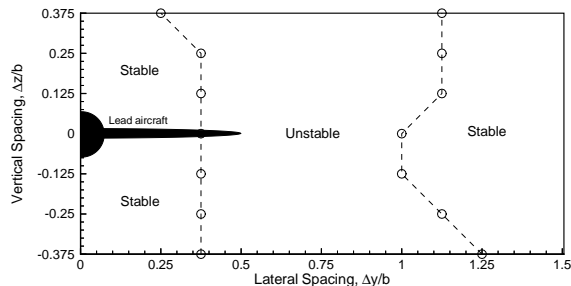


FIGURE 20. Measured regions of positional stability in roll,  $x/b=2$ .

In all three cases, there is a break in the stable regions at about 0.40 span spacing. For the basic horseshoe vortex model of a wing, this is the spacing where vortex systems of the wing no longer overlap in the spanwise direction, i.e., the trailing vortex of the downstream wing moves outboard of the trailing vortex of the wing upstream.

### CONCLUSION

Results from a wind tunnel test of two vertical tailless delta wing aircraft in close proximity have been presented and compared with predictions from a planar vortex lattice method. The relative positions of the aircraft were varied in the spanwise and vertical directions at a longitudinal separation of two wing spans from nose to nose. Wake induced effects on lift were large, and well predicted except when the aircraft overlapped in the spanwise direction. In that case, the lift increments were overpredicted. Wake induced effects on pitching and rolling moment were large, and well predicted in all cases. Wake induced effects on side force and yawing moment were small, presumably due to the lack of a vertical tail. The induced drag on the trail aircraft was reduced when the aircraft wing tips were aligned or slightly overlapped. Drag increases were found when the

wing tips overlapped by more than 50% span. A maximum induced drag reduction of 25% was measured on the trail aircraft with a wing tip overlap of 15-20% span. This compares with a predicted reduction of 40% with 10% overlap. The discrepancy was attributed to flow separation at the tip caused by upwash.

### REFERENCES

1. Hoerner, S.F., "Fluid Dynamic Drag," published by the author, 1965.
2. Lissaman, P.B.S., and Shollenberger, C.A., "Formation Flight of Birds," Science, Vol. 168, pp. 1003-1005, 22 May 1970.
3. Hainsworth, F.R., "Precision and Dynamics of Positioning by Canada Geese Flying in Formation," Journal of Experimental Biology, Vol. 128, pp. 445-462, 1987.
4. Maskew, B., "Formation Flying Benefits Based on Vortex Lattice Calculations," NASA CR-151974, May 1977.
5. Blake, W.B., and Multhopp, D, "Design, Performance and Modeling Considerations for Close Formation Flight," AIAA paper 98-4343, presented at the AIAA Atmospheric Flight Mechanics Conference, Boston MA, August 1998.
6. Brown, C.E., Van Dyke, P, and Kloetzli, J.W., "Measurements and Analysis of the Forces Acting on a Small Aircraft Flying in the Upwash of a Large Aircraft," Tracor Hydronautics Technical Report 7615, April 1978.
7. Beukenberg, M. and Hummel, D., "Aerodynamics, Performance and Control of Airplanes in Formation Flight," ICAS paper 90-5.9.3, 1990.
8. Rossow, V.J., Sacco, J.N., Askins, P.A., Bisbee, L.S., and Smith, S.M., "Measurements in 80 by 120 Foot Wind Tunnel of Hazard Posed by Lift-Generated Wakes," Journal of Aircraft, Vol. 32, No. 2, pp. 278-284, August 1993.
9. Pete, K.R., Smith, S.T., and Vicroy, D.D., "Model Validation of Wake-Vortex/Aircraft

Encounters,” AIAA paper 2000-3979, presented at the AIAA Atmospheric Flight Mechanics Conference, Denver CO, August 2000.

10. Bloy, A.W., West, M.G., Lea, K.A., Jouma’a, M., “Lateral Aerodynamic Interference Between Tanker and Receiver in Aor-to-Air Refueling,” Journal of Aircraft, Vol. 30, No. 5, pp. 705-710, September-October 1993.

11. Gingras, D.R., “Experimental Investigation of a Multi-Aircraft Formation,” AIAA paper 99-3143, presented at the AIAA Applied Aerodynamics Conference, Norfolk VA, June-July 1999.

12. Albright, A.E., Dixon, C.J., and Hegedus, M.C., “Modification and Validation of Conceptual Design Aerodynamic Prediction Method HASC95 With VTXCHN,” NASA CR-4712, March 1996.

13. Rossow, V.J., “Validation of Vortex-Lattice Method for Loads on Wings in Lift-Generated Wakes,” Journal of Aircraft, Vol. 32, No. 6, November-December 1995, pp. 1254-1262.

14. Addington, G.A., and Myatt, J.H., “Control Surface Deflection Effects on Aerodynamic Response Nonlinearities,” AIAA paper 2000-4107, presented at the AIAA Atmospheric Flight Mechanics Conference, August 2000.

15. Gillard, W.J., and Dorsett, K.M., “Directional Control for Tailless Aircraft Using All Moving Wing Tips,” AIAA paper 97-3487, presented at the AIAA Atmospheric Flight Mechanics Conference, August 1997.

16. Prandtl, L., “Induced Drag of Multiplanes,” NACA TN 182, March 1924.

## APPENDIX – LONGITUDINAL DYNAMIC ANALYSIS

For formation flight, the longitudinal equations of motion can be expanded to include the effects of vertical position as follows:

$$\begin{bmatrix} -2D_o/u_o & (g-D\alpha)/u_o & 0 & -g & 0 \\ -2g/u_o & -L\alpha/u_o & u_o & -L\theta & -L_z \\ 0 & M\alpha/u_o & M_q & M_\theta & M_z \\ 0 & 0 & 1 & 0 & 0 \\ 0 & -1 & 0 & u_o & 0 \end{bmatrix} \begin{bmatrix} u \\ w \\ q \\ \theta \\ z \end{bmatrix} = \begin{bmatrix} \dot{u} \\ \dot{w} \\ \dot{q} \\ \dot{\theta} \\ \dot{z} \end{bmatrix}$$

with:

$$D_o = \frac{qS}{m} C_D \quad D\alpha = \frac{qS}{m} C_{D\alpha} \quad L\alpha = \frac{qS}{m} C_{L\alpha} \quad L\theta = \frac{qS}{m} C_{L\theta} \quad L_z = \frac{qS}{m} C_{Lz}$$

$$M\alpha = \frac{qSc}{I_Y} C_{m\alpha} \quad M_q = \frac{qSc}{I_Y} \frac{c}{2V} C_{mq} \quad M_\theta = \frac{qSc}{I_Y} C_{m\theta} \quad M_z = \frac{qSc}{I_Y} C_{mz}$$

The characteristic equation of this system is of fifth order with the following coefficients:

$$s^5 : 1$$

$$s^4 : -M_q + \frac{L\alpha + 2D_o}{u_o}$$

$$s^3 : \frac{-L\alpha M_q}{u_o} + \frac{2D_o}{u_o} \left( \frac{L\alpha}{u_o} - M_q \right) + \frac{2g}{u_o^2} (g - D\alpha) - (M\alpha + M_\theta) - L_z$$

$$s^2 : \frac{-2}{u_o^2} M_q [g(g - D\alpha) + L\alpha D_o] - \frac{2}{u_o} D_o (L_z + M\alpha + M_\theta) + \frac{1}{u_o} (M\alpha L\theta - L\alpha M_\theta) + L_z M_q$$

$$s^1 : \frac{-2g^2}{u_o^2} M\alpha + \frac{2}{u_o^2} [D_o (M\alpha L\theta - L\alpha M_\theta) - M_\theta g (g - D\alpha)] + \frac{2}{u_o} D_o L_z M_q + L_z (M\alpha + M_\theta) - M_z (L\alpha + L\theta)$$

$$s^0 : \frac{2}{u_o} D_o [L_z (M\alpha + M_\theta) - M_z (L\alpha + L\theta)] + \frac{2}{u_o} g D\alpha M_z$$

The formation terms add one aperiodic mode to the system. For stability, a necessary (but not sufficient) condition is that each of the  $s^n$  coefficients be positive. A quick inspection shows that for the formation derivatives to be stabilizing,  $L_z$  and  $M_\theta$  should be negative while  $L\theta$  should be positive.  $M_z$ , which only appears in the  $s^0$  and  $s^1$  coefficients, presents an interesting case. Intuitively, one might expect a negative value is desired, i.e. the aircraft will tend to pitch towards its original flight path once disturbed. This is the case for the  $s^1$  coefficient. For the  $s^0$  term, however, a negative value is destabilizing for the following condition:

$$C_L C_{D\alpha} > C_D (C_{L\alpha} + C_{L\theta})$$

Assuming a parabolic drag polar and  $C_{L\theta} = 0$ , this condition is satisfied if the lift coefficient is larger

than that corresponding to the maximum lift to drag ratio, i.e.:

$$C_L > \sqrt{\pi AR C_{D_o}}$$

Numerical results were generated for a full scale version of the tailless aircraft ( $b=37.5$  ft) using wind tunnel derived stability derivatives. Pitch damping was computed using HASC95. Two flight conditions were examined,  $M=0.6$  at 10,000 and 30,000 ft. These bracket the effect of  $M_z$  on the  $s^0$  term. The analysis was conducted with the formation specific derivatives varied one at a time, at their maximum values, shown below:

$$C_{Lz} = \pm 0.0053, 1/ft \quad @ y/b = 0$$

$$C_{mz} = \pm 0.0017, 1/ft \quad @ y/b = 0$$

$$C_{L\theta} = -0.138, 1/rad \quad @ y/b = 0.8125$$

$$C_{m\theta} = 0.046, 1/rad \quad @ y/b = 0.8125$$

Eigenvalues for sample calculation, M=0.6, 30,000 ft

$C_{Lz}$	$C_{mz}$	$C_{L\theta}$	$C_{m\theta}$	$\lambda_{1,2}$ (short period)	$\lambda_{3,4}$ (phugiod)	$\lambda_5$
-0.005	0	0	0	-0.729 $\gamma$ 1.172i	-0.012 $\gamma$ 0.671i	-0.013
0				-0.744 $\gamma$ 1.077i	-0.004 $\gamma$ 0.065i	0
0.005				-0.711 $\gamma$ 1.000i	-0.779, -0.013	0.719
0	-0.002	0	0	-1.914 $\gamma$ 1.718i	1.163 $\gamma$ 1.636i	0.005
	0			-0.744 $\gamma$ 1.077i	-0.004 $\gamma$ 0.065i	0
	0.002			-0.416 $\gamma$ 2.369i	-2.505, 0.005	1.837
0	0	-0.138	0	-0.732 $\gamma$ 1.072i	-0.015 $\gamma$ 0.066i	0
0	0	0	0.046	-0.775, -1.690	-0.002, 0.971	0

Eigenvalues for sample calculation, M=0.6, 10,000 ft

$C_{Lz}$	$C_{mz}$	$C_{L\theta}$	$C_{m\theta}$	$\lambda_{1,2}$ (short period)	$\lambda_{3,4}$ (phugiod)	$\lambda_5$
-0.005	0	0	0	-1.555 $\gamma$ 1.647i	-0.030 $\gamma$ 0.622i	-0.014
0				-1.585 $\gamma$ 1.584i	-0.007 $\gamma$ 0.053i	0
0.005				-1.606 $\gamma$ 1.517i	-0.014, -0.613	0.655
0	-0.002	0	0	-2.712 $\gamma$ 2.198i	1.127 $\gamma$ 1.948i	-0.014
	0			-1.585 $\gamma$ 1.584i	-0.007 $\gamma$ 0.053i	0
	0.002			-0.921 $\gamma$ 2.898i	-3.331, -0.014	2.002
0	0	-0.138	0	-1.585 $\gamma$ 1.584i	-0.007 $\gamma$ 0.053i	0
0	0	0	0.046	-1.885 $\gamma$ 0.958i	-0.013, 0.599	0

The results are shown above. The height stability derivative  $C_{Lz}$  has no effect on the short period characteristics. It does affect the phugoid, with an unstable value changing the response to two aperiodic modes, both of which are stable. The primary effect of  $C_{Lz}$  is to add a new mode. For a positive value of  $C_{Lz}$ , the new mode is unstable with a time to double amplitude of about 1 second.

The lift derivative  $C_{L\theta}$  has almost no effect on the dynamic modes. It almost always appears summed with the lift curve slope,  $C_{L\alpha}$ , in the characteristic equation. It is only 6% of the magnitude of the lift curve slope, however, so its contribution would be expected to be very small.

The moment derivative  $C_{mz}$  has a major effect on all of the derivatives. Although the short period remains stable for all values of  $C_{mz}$ , the damping is significantly reduced for positive  $C_{mz}$ . Negative values of  $C_{mz}$  cause the phugoid to go unstable, with a time to double amplitude of about 0.6 sec. Positive values drive the phugoid root to an aperiodic pair. The new mode is unstable for positive  $C_{mz}$ , with a time to double amplitude of 1/3 sec. The effect of negative  $C_{mz}$  on the new mode is a function of the flight condition, as hypothesized

by the analysis of the coefficients of the characteristic equation. None of the  $C_{mz}$  values studied result in a completely stable system.

The effect of the moment derivative  $C_{m\theta}$  is flight condition dependent. As with  $C_{L\theta}$ , it almost always appears summed with the pitch stiffness,  $C_{m\alpha}$ , in the characteristic equation. However, it is twice the magnitude  $C_{m\alpha}$ , so it has a significant impact. It drives the phugoid mode to two aperiodic roots, one unstable with a time to double amplitude of about 1 second. For the low altitude flight condition, it increases the short period damping, and for the high altitude condition, it drives the short period to two stable aperiodic roots.

If the derivatives were varied in combination with each other and not one at a time, their effects on the dynamic modes would probably change.